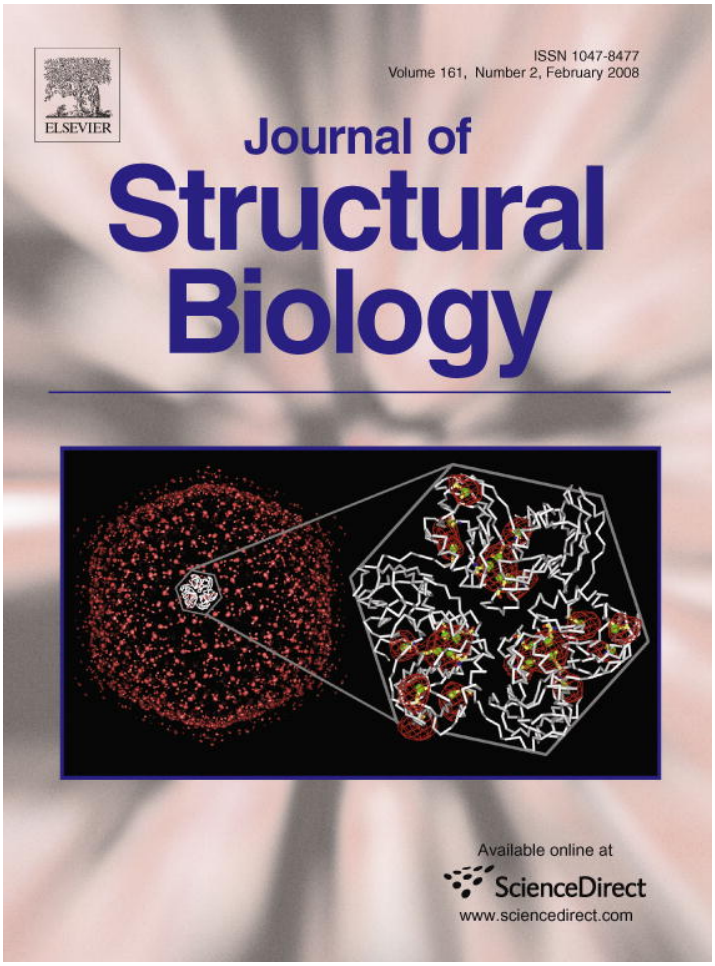

Available online at www.sciencedirect.com
ScienceDirect
Journal of Structural Biology 161 (2008) 151–161
Journal of Structural Biology
www.elsevier.com/locate/yjsbi

The effect of peptide glycation on local secondary structure

Jane F. Povey [1], Mark J. Howard [1], Richard A. Williamson, C. Mark Smales *

Protein Science Group, Department of Biosciences, University of Kent, Canterbury, Kent CT2 7NJ, UK

Received 16 May 2007; received in revised form 28 September 2007; accepted 10 October 2007
Available online 17 October 2007

Abstract

Protein glycation is a non-enzymatic reaction between reducing sugars and amino groups that occurs *in vivo* and has been implicated in a number of disease states and pathologies including Alzheimer's and diabetes. Although glycation is thought to alter protein structure and function, there is currently little information on the structural consequences of this modification. We have used a model α-helix and a model β-hairpin peptide, and NMR analysis, to investigate the effects of glycation upon secondary structure. Glycation of the dilysine motif within the α-helix peptide occurred preferentially at one lysine residue and resulted in severe disruption to the local secondary structure. The area immediately around the site of modification was extremely flexible and the peptide did not adopt a preferred conformation in this area of the helix in 30% TFE. Significant glycation of the β-hairpin peptide was not detected and the structure was unchanged. These results show that glycation results in local secondary structure distortion of α-helices and that preferential glycation occurs in a sequence specific manner. The findings will allow us to interrogate the local environment in other peptides/proteins to predict the likelihood of glycation, and to model the potential effects such modification might have upon structure/function.

Keywords: NMR; Glycation; Peptide secondary structure; α-Helix; β-Turn

1. Introduction

Non-enzymatic glycation of proteins has been shown to be a potential problem during their storage in the food and biotech industries (Davis et al., 2001; Smales et al., 2002), and also in human health as a complication of diseases such as diabetes (Al-Abed et al., 1999; Stitt, 2001). Glycation occurs *via* the Maillard reaction in which a reducing sugar reacts with an amino group on a protein, either at the NH_2 terminus or at the ε-amino group of lysine residues (Tagami et al., 2000; Yeboah et al., 2004). This results in the formation of Amadori products for reaction with glucose (Bucala, 1996) or Heyns products for reaction with fructose (Suarez et al., 1989). These adducts can then further react and rearrange to give a spectrum of products known as Advanced Glycation End products or AGEs (Cohen, 2003).

Many foodstuffs and biotech products are necessarily processed and stored in the presence of sugars to aid in maintaining protein integrity (Smales et al., 2000). Non-enzymatic glycation and subsequent AGE formation of such products may affect protein structure, function and immunogenicity (Howard and Smales, 2005). Although these reactions and the effects of these modifications on protein function have been studied for several decades, prediction of where modification may take place, or of the effect on protein structure, remains largely unknown. A better understanding of those residues, protein sequences or structures that are prone to modification, and the effect of this modification on structure and ultimately function, will allow the development of approaches to protect against or limit these potentially harmful modifications.

Despite all the interest in non-enzymatic glycation, until recently very little was known about the detailed structural changes that occur within either the modified protein or at

* Corresponding author. Fax: +44 01227 763912.
E-mail address: c.m.smales@kent.ac.uk (C.M. Smales).
[1] These authors contributed equally to this work.

1047-8477/$ - see front matter © 2007 Elsevier Inc. All rights reserved.
doi:10.1016/j.jsb.2007.10.004

the secondary structure level. Certainly, it has been reported that glycation and subsequent AGE formation can give rise to protein aggregation, interaction with other proteins and lead to the inactivation of enzymes (Yeboah et al., 2004). More recently we used NMR and a model helical peptide from human serum albumin (HSA) to show that glycation with glucose caused the helical nature of the peptide to be distorted around the region of the site of modification (Howard and Smales, 2005). This study also showed that preferential glycation of one lysine residue within a dilysine motif occurred, in agreement with previous studies that have shown this to be the case in the intact protein (Iberg and Flückiger, 1986). This preferential glycation appears to be the result of the surrounding environment that leaves one lysine amino group more nucleophilic than its neighbor. In one of the few other studies that have looked at protein glycation in a structural context, Mendez et al. (2005) investigated how non-enzymatic glycation affected the secondary and tertiary structures of intact HSA (Mendez et al., 2005). Using CD and fluorescence-based methods they showed that there was some perturbation of local structure following glycation but that the overall structure of the protein remained unchanged, although these methods have relatively low structural resolution.

Here, we have extended our previous NMR based study (Howard and Smales, 2005) to determine if perturbation in local secondary structure upon glycation is conserved across different helical peptides and in other secondary structures. Specifically, we have investigated the effect of non-enzymatic glycation on a helical peptide from hen egg white lysozyme (helix 4) that has previously been shown to be glycated (Tagami et al., 2000). The peptide also contains a dilysine motif and in the intact protein one of these lysine's is preferentially glycated (Smales et al., 2000). We also investigated a second model peptide forming a different secondary structure corresponding to the AB turn region of tissue inhibitor of metalloproteinases-2 (TIMP-2) (Muskett et al., 1998). This peptide contains only a single lysine residue allowing us to investigate whether a single lysine is as susceptible to glycation and further, whether glycation resulted in secondary structure distortion in a similar manner to that observed in helical peptides.

Using the lysozyme model peptide and NMR analysis in the presence of 30% trifluoroethanol (TFE) we have shown that the unmodified peptide forms a helix similar to that in the intact protein but that upon glycation the structure of this helix is considerably disrupted in the region of the modification. One lysine was preferentially glycated over the other in agreement with the data for intact lysozyme (Smales et al., 2000). Significant glycation of the TIMP-2 AB β-hairpin peptide was not detected, although this peptide contains only a single lysine residue. The structure of the peptide before and after the glycation reaction was identical and representative of the equivalent region in the intact TIMP-2 protein. Collectively our results show that glycation results in local secondary structure distortion of α-helices and that preferential glycation occurs in a sequence specific manner. The results of this investigation will allow investigators to predict the likely sites of protein glycation in intact proteins and model the possible effect on local secondary structure. Such knowledge will help aid the development of novel strategies to limit or eliminate these potentially damaging reactions. As such we discuss our results in terms of both the structure/function consequences and bioprocessing of therapeutic or food-based proteins.

2. Materials and methods

All materials were of analytical reagent grade or better and purchased from Sigma Aldrich unless otherwise stated.

2.1. Synthesis and purification of the peptides corresponding to hen egg white lysozyme helix 4 and tissue inhibitor of metalloproteinases-2 (TIMP-2) β-hairpin between strands A and B

The peptides SDPTASVNCAKKIVSDGNGM (lysozyme helix 4) and CVDSGNDIYGNPIKRC (TIMP-2 β-hairpin between strands A and B) were synthesized using a Shimadzu PSSM-8 Multiple Peptide Synthesizer and an fmoc/HBTu synthesis strategy. The termini of peptides were in an unprotected state for all experiments. The TIMP-2 AB β-hairpin peptide was oxidized for 6 days in ammonium bicarbonate buffer to ensure that disulphide bond formation was complete. The resulting peptides were purified by reverse-phase HPLC using a preparative C_{18} 10×250 mm column linked to a Waters series HPLC machine. The peptides were injected onto the column and salts washed out with 10% acetonitrile containing 0.05% TFA. The peptides were then eluted from the column using a linear gradient from 10 to 70% acetonitrile (containing 0.045% TFA) over 45 min. The peptide peaks were collected and freeze-dried overnight. Multiple runs were combined in order to purify each of the synthesized peptides. The authenticities of the purified peptides were confirmed by electrospray mass spectrometry. Mass spectra were recorded in the positive ion mode using the extended mass range (m/z 250–4000) on a Finnigan MAT LCQ ion-trap mass spectrometer.

2.2. Glycation of the synthetic lysozyme and TIMP-2 peptides

Glycated peptide was generated using the conditions and procedures previously described (Howard and Smales, 2005).

2.3. NMR sample preparation

For NMR analysis peptide samples were prepared as previously described (Povey et al., 2007), except in the case

of the TIMP-2 AB β-hairpin peptide whereby TFE was omitted from the sample.

2.4. NMR spectroscopy

All experiments were recorded on a Varian UnityINOVA 600 MHz NMR spectrometer with a z-shielded gradient triple resonance probe using standard procedures, essentially as previously described (Howard and Smales, 2005). The lysozyme peptide experiments were recorded at 10 °C and the TIMP-2 AB β-hairpin peptide experiments were run and recorded at 0 °C. For each peptide sample, a two-dimensional nuclear Overhauser effect spectroscopy (NOESY) and total correlation spectroscopy (TOCSY) experiment was recorded with mixing times of 250 and 80 ms, respectively. These experiments were collected with 512 and 2048 complex points with acquisition times of 79 and 315 ms in the indirectly and directly acquired ^{1}H dimensions, respectively. Data processing and analysis were carried out on using NMRPipe (Delaglio et al., 1995) and NMRView (Johnson and Blevins, 1994), respectively. All chemical shifts were referenced externally to a 100 μM solution of dimethylsilapetane sulphonic acid (DSS) in PBS containing 30% (v/v) TFE for lysozyme helix four experiments and to a 100 μM solution of dimethylsilapetane sulphonic acid (DSS) in PBS for the TIMP-2 AB hairpin experiments.

2.5. Structural calculations and analysis

All structural calculations were undertaken using the Crystallography and NMR System (CNS) version 1.1 (Brunger et al., 1998) running on Silicon Graphics O2+ and Transtec X2100 Linux workstations. CNS parameter files were modified to incorporate the covalent structure of the modified lysine residue for calculations. All NOE contacts were grouped into one wide classification between 1.8 and 5.0 Å with final structures calculated from extended coordinates using the standard CNS NMR anneal protocol with sum averaging for dynamic annealing with NOEs from both extended and folded precursors (Brunger et al., 1998). We chose not to classify the NOEs into different classes in order to be careful not to give any one NOE more influence over another. H-bond donor receptor pairs and secondary structure ϕ restrains were deduced from the initial structural calculations and then subsequently used during the refinement of the final ensembles. Final structural ensembles of 40 structures for each lysozyme helix 4, and 30 structures for each TIMP-2 AB β-hairpin peptide, were produced with all structures used to produce statistical energy and root mean square (rms) deviation structural information. Backbone and heavy atom rms deviation values were obtained using MOLMOL version 2k.2 (Koradi et al., 1996). The structural integrity of each ensemble was evaluated using PROCHECK-NMR (Laskowski et al., 1996). The comparison of the energies between the calculated structures determined in this work and the equivalent helix from lysozyme and turn from TIMP-2 were undertaken using GROMOS96 43B1 parameter set (van Gunsteren et al., 1994) within DEEPVIEW version 3.7 (Guex and Peitsch, 1997).

3. Results

3.1. Peptide synthesis, glycation and purification

The peptide sequences corresponding to lysozyme α-helix 4 (residues 86–105) and TIMP-2 AB β-hairpin (residues 29–42) were successfully synthesized on a Shimadzu PSSM-8 Multiple Peptide Synthesizer as determined by mass spectrometry. The peptide sequence of the helix was identical to that found in the native lysozyme molecule except that the third residue Ile^{88} was deliberately replaced with a proline residue (calculated mass = 1993.0 Da, experimental mass = 1993.9 Da). The peptide sequence for the TIMP-2 AB β-hairpin was identical to that found in the native TIMP-2 molecule except for the addition of a cysteine residue at each end of the peptide. These cysteine residues were oxidized to form a disulphide bridge, formation of which was once again confirmed by mass spectrometry (calculated mass = 1750.8 Da, experimental mass = 1751.7 Da).

3.2. NMR resonance assignments

Spin systems were identified by analysis of two-dimensional TOCSY NMR spectra and all the observed ^{1}H chemical shifts are listed in Tables 1 and 2 for the lysozyme helix and TIMP-2 AB β-hairpin peptides, respectively. Almost all ^{1}H spin systems were assigned for the unmodified and modified peptide for lysozyme helix 4 and TIMP-2 AB β-hairpin as described in Tables 1 and 2.

The TOCSY NMR spectra of the lysozyme helix 4 peptide after glycation contained a defined 'sugar box' region corresponding to peaks derived from the attached sugar residue which, as expected, was absent from the control unmodified peptide (Fig. 1A v Fig. 1B). As this peptide contains two lysine residues, it was necessary to determine whether one of these residues was preferentially glycated or if there was a mixed population of monoglycated peptides and diglycated material present. Determination and assignment of the glycated lysine residue in lysozyme helix 4 was undertaken by direct comparison of the changes in the spectra before and after modification. Both Lys^{96} and Lys^{97} were unambiguously identified using NOE data in the spectra of the unmodified peptide. Following modification there was a marked change in the H^{α} chemical shift for Lys^{97} but not Lys^{96} (see Table 1 and Fig. 2A). Interestingly, while the H^{α} chemical shift of Lys^{96} showed no change in the glycated form the other residues directly adjacent to the two Lys residues (Cys^{94} and Ile^{98}) showed a large change in the chemical shift in the modified form (Table 1 and Fig. 2A). Investigation of the chemical shifts for each of the protons within the two lysine residues once again

Table 1
Helix 4 NMR assignment list of observed ^{1}H chemical shifts for the unmodified and Amadori modified peptide in PBS containing 30% (v/v) TFE at 10 °C

Residue	H^N	H^α	Others
86 Ser		4.00	$H^{\beta1/\beta2}$ 3.79/3.87
87 Asp	8.70	4.91	$H^{\beta1/\beta2}$ 2.76/2.59
*Pro		4.37	$H^{\beta1}$ 2.23, $H^{\gamma1}$ 1.94, $H^{\delta1}$ 3.78
89 Thr	8.05	4.15	$H^{\beta1}$ 4.04, $H^{\gamma21}$ 1.11
90 Ala	7.31	4.15	$H^{\beta1}$ 1.35
91 Ser	7.97	4.24	$H^{\beta1/\beta2}$ 3.87/3.78
92 Val	7.86	3.80	$H^{\beta1}$ 2.01, $H^{\gamma11/\gamma21}$ 0.82/0.87
93 Asn	8.12	4.48	$H^{\beta1}$ 2.70, $H^{\delta21/\delta22}$ 7.46/6.76
94 Cys	7.99	4.18	$H^{\beta1/\beta2}$ 2.88/2.86
95 Ala	8.03	3.97	$H^{\beta1}$ 1.34
96 Lys	8.03	3.93	$H^{\beta1/\beta2}$ 1.73/1.57, $H^{\gamma1/\gamma2}$ 1.28/1.46, $H^{\delta1}$1.56, $H^{\varepsilon1}$ 2.82
97 Lys	7.56	4.02	$H^{\beta1/\beta2}$ 1.69/1.81, $H^{\gamma1/\gamma2}$ 1.30/1.37, $H^{\delta1}$ 1.56, $H^{\varepsilon1}$ 2.86
98 Ile	7.87	3.53	$H^{\beta1}$ 1.82, $H^{\gamma11/\gamma21/\gamma12}$ 1.03/0.77/1.52, $H^{\delta1}$ 0.72
99 Val	8.08	3.84	$H^{\beta1}$ 2.00, $H^{\gamma11/\gamma21}$ 0.82/0.87
100 Ser	7.99	4.28	$H^{\beta1}$ 3.86
101 Asp	8.21	4.59	$H^{\beta1}$ 2.81
102 Gly	8.16	3.85	
103 Asn	8.07	4.63	$H^{\beta1}$ 2.73, $H^{\delta21/\delta22}$ 7.45/6.70
104 Gly	8.28	3.87/3.77	
105 Met	7.78	4.31	$H^{\beta1/\beta2}$ 1.87/2.02, $H^{\gamma1/\gamma2}$ 2.35/2.42
Modified peptide			
86 Ser		4.02	$H^{\beta1/\beta2}$ 3.88/3.80
87 Asp	8.70	4.91	$H^{\beta1/\beta2}$ 2.76/2.58
*Pro		4.39	$H^{\beta1/\beta2}$ 2.24/1.93, $H^{\gamma1}$ 1.94, $H^{\delta1}$ 3.81
89 Thr	8.13	4.16	$H^{\beta1}$ 4.02, $H^{\gamma1}$ 1.12
90 Ala	7.86	4.15	$H^{\beta1}$ 1.36
91 Ser	7.97	4.21	$H^{\beta1}$ 3.78
92 Val	7.84	3.80	$H^{\beta1}$ 2.00, $H^{\gamma11/\gamma21}$ 0.88/0.83
93 Asn	8.16	4.47	$H^{\beta1}$ 4.92, $H^{\delta21/\delta22}$ 5.89/5.43
94 Cys	8.15	4.43	$H^{\beta1/\beta2}$ 3.02/3.06
95 Ala	8.07	4.00	$H^{\beta1}$ 1.34
96 Lys	7.99	3.92	$H^{\beta1/\beta2}$1.74/1.66, $H^{\gamma1/\gamma2}$ 1.30/1.39, $H^{\delta1}$ 1.57, $H^{\varepsilon1}$ 2.85
97 Lys	7.86	4.20	$H^{\beta1/\beta2}$ 2.19/1.75, $H^{\gamma2}$ 1.50, $H^{\delta1}$ 2.00, $H^{\varepsilon1}$ 2.75, $H^{\zeta2}$ 5.10, $H^{\kappa2}$ 3.60, $H^{\gamma2}$ 3.70, $H^{\mu2}/^{\mu3}$ 3.30/3.40
98 Ile	7.97	3.83	$H^{\beta1}$ 1.83, $H^{\gamma11/\gamma21/\gamma12}$1.01/0.77/1.25, $H^{\delta31}$ 0.72
99 Val	8.10	3.84	$H^{\beta1}$ 2.02, $H^{\gamma11/\gamma21}$ 0.83/0.89
100 Ser	7.99	4.28	$H^{\beta1}$ 3.82
101 Asp	8.22	4.58	$H^{\beta1}$ 2.79
102 Gly	8.15	3.86	
103 Asn	8.08	4.64	$H^{\beta1}$ 2.75, $H^{\delta22/\delta21}$ 6.72/7.47
104 Gly	8.30	3.87/3.78	
105 Met	7.75	4.28	$H^{\beta1/\beta2}$ 1.87/2.02, $H^{\gamma1/\gamma2}$ 2.43/2.36

All chemical shifts are referenced externally to a 100 μM solution of dimethylsilapetane sulphonic acid (DSS) in PBS containing 30% (v/v) TFE. Key: *Ile^{88} in lysozyme → Pro in model peptide.

showed that in the modified peptide Lys^{96} chemical shifts were unchanged from the native whilst those of Lys^{97} showed large changes (Fig. 3). This was also confirmed by CSI analysis of the chemical shift data (data not shown).

The TOCSY NMR spectra of the TIMP-2 AB β-hairpin after glycation did contain a weak and less well defined 'sugar box' compared to the control unmodified peptide (Fig. 1C v Fig. 1D), suggesting that limited glycation had occurred. This peptide contains only one lysine residue (Lys^{41}), which was unambiguously identified using NOE data in the spectra of the unmodified peptide. Following subjection of the peptide to conditions that should result in modification there was no observable change in the H^α chemical shifts of Lys^{41} and the H shifts for the rest of the sidechain remained more-or-less unchanged between the modified and unmodified peptide (see Table 2). Further, there was relatively little change in the H^α chemical shifts throughout the entire TIMP-2 AB β-hairpin peptide following glycation (Table 2 and Fig. 2B), suggesting that glycation had occurred on only a very small proportion of the peptide molecules, or alternatively, that glycation had no effect on the structure under the conditions that the data was collected.

3.3. Structural assignments and additional restraints

Through-space assignments were achieved using two-dimensional NOESY spectra of the unmodified and glycat-

Table 2
TIMP-2 AB β-hairpin NMR assignment list of observed ^{1}H chemical shifts for the unmodified and Amadori modified peptide in PBS at 0 °C

Residue	H^N	H^α	Others
Cys		4.16	$H^{\beta1/\beta2}$ 2.90/2.93
29 Val	8.58	4.01	$H^{\beta1}$ 1.77, H $^{\gamma11}$ 0.65
30 Asp	8.53	4.48	$H^{\beta1/\beta2}$ 2.39/2.54
31 Ser	8.18	4.25	H $^{\beta1}$ 3.53
32 Gly	8.16	3.54/3.87	
33 Asn	8.30	5.08	$H^{\beta1/\beta2}$ 2.09/2.30, $H^{\delta21/\delta22}$ 7.24/6.52
34 Asp	8.80	4.30	$H^{\beta1/\beta2}$ 2.41/3.03
35 He	7.79	3.68	$H^{\beta1}$ 1.42, H $^{\gamma11/\gamma12\ \gamma21/}$ 0.37/0.59/0.35, $H^{\delta1}$ 0.24
36 Tyr	7.68	4.28	$H^{\beta1/\beta2}$ 2.66/3.02, $H^{\delta1/\delta1}$ 6.51/6.81
37 Gly	7.88	3.30/3.95	
38 Asn	8.20	4.84	$H^{\beta1/\beta2}$ 2.42/2.61
39 Pro		4.50	$H^{\beta1/\beta2}$ 1.72/2.00, $H^{\gamma1}$ 1.54, $H^{\delta1\delta1/}$ 3.45/3.62
40 Ile	8.17	3.74	$H^{\beta1}$ 1.34, $H^{\gamma11/\gamma21/\gamma12}$ 0.74/0.59/1.19, $H^{\delta1}$ 0.50
41 Lys	8.36	4.21	$H^{\beta1/\beta2}$ 1.39/1.48, $H^{\gamma1/\gamma2}$ 1.06/1.12
42 Arg	8.43	4.23	$H^{\beta1\ \beta1/}$ 1.47/1.60, $H^{\gamma1}$ 1.35, $H^{\delta1}$ 2.90, $H^{\varepsilon1}$ 6.99
Cys	8.31	4.21	$H^{\beta1/\beta2}$ 2.70/2.95
Modified peptide			
Cys		4.16	$H^{\beta1/\beta2}$ 2.89/2.94
29 Val	8.58	4.00	$H^{\beta1}$ 1.77, $H^{\gamma11}$ 0.64
30 Asp	8.58	4.51	$H^{\beta1/\beta2}$ 2.45/2.60
31 Ser	8.19	4.23	$H^{\beta1}$ 3.54
32 Gly	8.13	3.55/3.85	
33 Asn	8.28	5.00	$H^{\beta1/\beta2}$ 2.14/2.30, $H^{\delta21/\delta22}$ 7.25/6.54
34 Asp	8.75	4.32	$H^{\beta1\ \beta1/}$ 2.43/2.99
35 Ile	7.80	3.68	$H^{\beta1}$ 1.42, $H^{\gamma11/\gamma12\ \gamma21/}$ 0.39/0.59/0.35
36 Tyr	7.71	4.27	$H^{\beta1/\beta2}$ 2.66/2.99, $H^{\delta1/\delta1}$ 6.51/6.81
37Gly	7.89	3.30/3.92	
38 Asn	8.15	4.82	$H^{\beta1/\beta2}$ 2.44/2.58, $H^{\delta21/\delta22}$ 6.94/6.80
39 Pro		4.48	$H^{\beta1/\beta2}$ 1.72/2.00, $H^{\gamma1}$ 1.55, $H^{\delta1\ \delta1/}$ 3.47/3.60
40 Ile	8.13	3.74	$H^{\beta1}$ 1.36, H $^{\gamma11/\gamma21/\gamma12}$ 0.75/0.52/1.19, $H^{\delta1}$ 0.58
41 Lys	8.31	4.20	$H^{\beta1/\beta2}$ 1.37/1.49, $H^{\gamma1/\gamma2}$ 1.06/1.11
42 Arg	8.29	4.22	$H^{\beta1\ \beta1/}$ 1.47/1.60, $H^{\gamma1}$ 1.35, $H^{\delta1}$2.90, $H^{\varepsilon1}$ 6.98
Cys	8.24	4.23	$H^{\beta1/\beta2}$ 2.72/2.95

All chemical shifts are referenced externally to a 100 μM solution of dimethylsilapetane sulphonic acid (DSS) in PBS.

ed peptides. The number of contact types with additional structural constraints are described in Tables 3 and 4 for the lysozyme helix 4 and TIMP-2 AB β-hairpin peptides, respectively. The distribution of restraints across each of the peptides in both the unmodified and glycated forms is depicted in Fig. 4. The NOE contact types observed in the unmodified lysozyme helix 4 (Fig. 4A) support the presence of an α-helix conformation with NOEs observed between Hα and HN (i–$i+3$) as well as Hα and Hβ (i–$i+3$). The NOE contact data in the glycated form of lysozyme helix 4, however, showed disruption of the NOE pattern consistent with a change in peptide conformation relative to the unmodified. There was little change between the NOE contact pattern of the unmodified and glycated TIMP-2 AB β-hairpin peptide (Fig. 4B).

3.4. Structure calculations and analysis of the unmodified and glycated lysozyme helix 4 peptides

All structural data were determined using CNS as described in the experimental procedures. No calculated structure gave violations greater than 0.2 Å or bond angle violations greater than 5° from the restraint data when all 40 structures were used to compute the ensemble average structural set. The rms deviation statistics for both the control and glycated lysozyme helix 4 peptides are shown in Table 5. The unmodified ensemble (Fig. 5a) resulted in good agreement between all calculated structures across the entire peptide and direct comparison of the calculated structure with the equivalent region in intact lysozyme (pdb IE8L) showed excellent agreement between the two structures (see Table 5). When the unmodified peptide structure is represented as a ribbon diagram, the helical nature of the peptide is observed (Fig. 5b). Energy comparisons between the models calculated here for the unmodified and glycated peptides, and the same region in the intact lysozyme structure, are shown in Table 6.

The rms deviation of the ensemble of the modified peptide showed a relatively poor agreement across the entire peptide, however each end of the structure showed much better agreement with the deviation occurring between residues 96–98 (Fig. 5c and Table 5). We note that the area of relatively poor agreement in the glycated peptide ensemble contains the modified Lys^{97} residue. When the calculated structure is represented as a ribbon diagram, loss of the helical nature of the peptide relative to the control is clearly

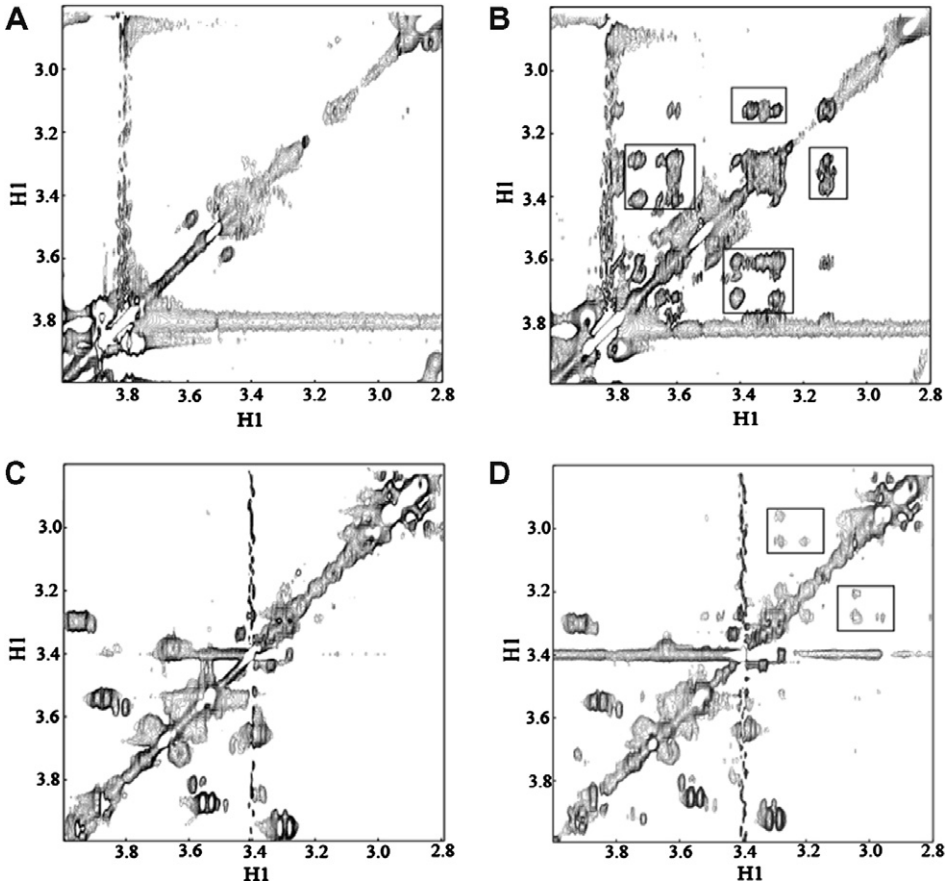

Fig. 1. Sugar box region of two-dimensional TOCSY NMR spectra for unmodified (A) and glycated (B) lysozyme helix 4 peptides and unmodified (C) and glycated (D) TIMP-2 AB β-hairpin peptides. The outlined regions show the resonances from the sugar nuclei. All assignments are illustrated in the format: [vertical (F1) ppm, horizontal (F2) ppm] and are for H^N unless stated.

visible within the region 96–98 and the helix appears to 'bend' slightly (Fig. 5d). We note that not only did each end of the modified peptide ensemble show good agreement between the structures, each end of the modified ensemble also matched the unmodified peptide ensemble (Table 5).

PROCHECK-NMR analysis of the Ramachandaran plot for the 40-structure ensemble of the control peptide showed that 98.3% of all residues fell in either the most favored or additionally allowed regions of the α-helix, with the remaining 1.7% falling in the generously allowed regions. Equivalent analysis of the glycated peptide showed 94.2% of all residues falling in the most favored or additionally allowed regions, with 4.8% falling into the generously allowed regions of the α-helix and the remaining 1% falling in disallowed regions.

3.5. Structure calculations and analysis of the TIMP-2 AB β-hairpin peptides

All structural data were determined as described for the lysozyme helix 4 peptide above. The rms deviation statistics from 30 structures for both the unmodified and glycated peptides are shown in Table 5. From the unmodified ensemble (Figs. 6A) it was clear that the two ends of the peptide showed a large amount of variation and this was reflected in the rms deviations across the entire peptide (Table 5). Removal of the two amino acids at each end of the peptide from the calculations resulted in much better agreement between all the calculated structures across the entire peptide and direct comparison of this region of the calculated structure with the equivalent region in intact TIMP-2 (pdb 2TMP) showed agreement between the two structures (see Table 5). Energy comparisons between the models calculated here for the unmodified and glycated peptides, and the same region in the intact TIMP-2 structure, are shown in Table 7.

The rms deviation of the ensemble of the modified peptide (Fig. 6B) showed greater variation across the entire peptide than the unmodified, although this once again improved by removal of the two residues at either end (Table 5). However, the structure of the peptide that had been subjected to glycation conditions appears to be unchanged compared to the control unmodified peptide and the rms deviations from direct comparison of the two confirmed this (Table 5). Overlaying the ensembles for both the control and modified peptides again showed these to be more-or-less equivalent (Fig. 6C). Comparison

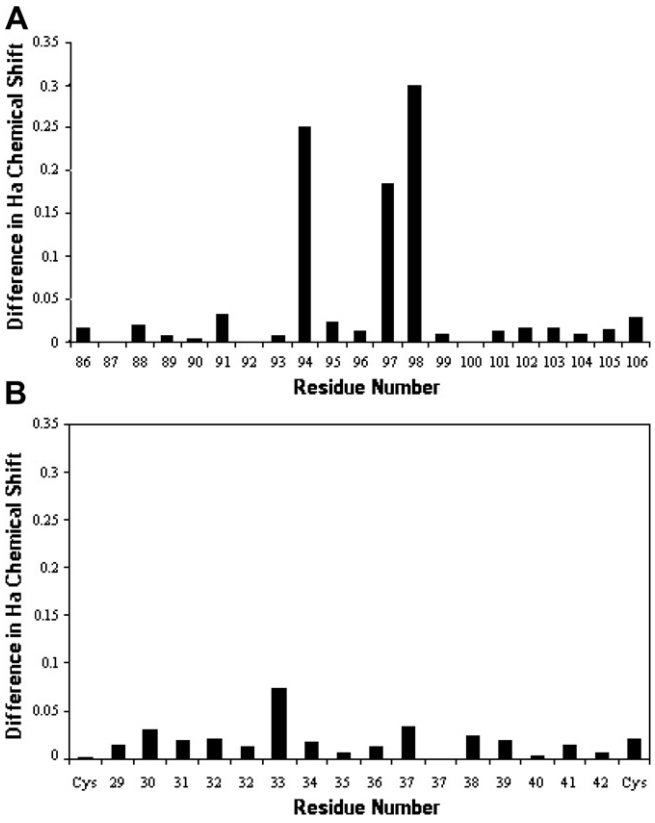

Fig. 2. Difference in ^{1}H NMR chemical shift observed between each residue in the unmodified and glycated peptides. (A) lysozyme helix 4, (B) TIMP-2 AB β-hairpin.

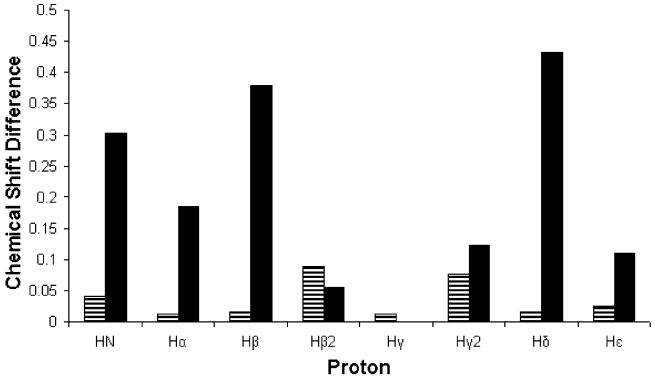

Fig. 3. Difference in NMR chemical shift observed for each assigned proton for the two lysine residues (Lys^{96} ▤, Lys^{97} ■) in lysozyme helix 4 between the unmodified and glycated peptides.

of both the peptides together with the equivalent TIMP-2 AB turn region extracted directly from the TIMP-2 NMR structure (Muskett et al., 1998) confirmed that the structures were all very similar (Fig. 6D) as shown by the rms deviation values (Table 5).

4. Discussion

The non-enzymatic reaction between reducing sugars and protein amino groups (glycation), and the advanced glycation end products (AGEs) derived from these glycation adducts, have now repeatedly been shown to cause enzyme inactivation, protein aggregation, and precipitation (Yeboah et al., 2004). Despite the importance of this protein modification, the effect(s) of glycation upon protein structure remain largely unknown. Recently we have used NMR to show that glycation of an HSA model peptide results in conformational distortion of the secondary structure (Howard and Smales, 2005). Here, we have used NMR to extend this investigation and describe the effect of glycation on the secondary structure of other model peptides.

NMR analysis of the modified lysozyme helix 4 peptide showed that glycation had indeed occurred and further, that this had occurred preferentially on Lys^{97}. This was confirmed by the lysine H$^{\alpha}$ chemical shift differences between the unmodified and glycated peptides and investigation of the chemical shifts for each of the protons within the two lysine residues (Fig. 3). Preferential glycation of Lys^{97} in the model peptide agrees with the intact protein data where it has previously been shown that Lys^{97} is preferentially glycated over Lys^{96} when modified under similar conditions (Smales et al., 2000). In the case of the intact protein, it is thought that preferential glycation occurs at this residue due to the relative surface accessibilities of the two NH_2 amino groups and local acid-base catalysis (Smales et al., 2000). Indeed, it has long been realized that glycation is more likely to occur on lysine residues which

Table 3
NOE, hydrogen bond and torsion angle connectives for both unmodified and glycated helix 4 peptide

		Unmodified peptide	Glycated peptide
NOE			
	Intra-residue	139	125
	Sequential	36	33
	i–$i+2$	4	3
	i–$i+3$	25	12
	i–j (>3)	6	3
	Total	210	176
Hydrogen bond donors		13	7
Torsion angles	ϕ	18	13

Table 4
NOE, hydrogen bond and torsion angle connectives for both unmodified and glycated TIMP-2 AB β-hairpin peptide

		Unmodified peptide	Glycated peptide
NOE			
Intra-residue		138	155
Sequential		34	35
i–$i+2$		5	7
i–$i+3$		1	0
i–j (>3)		25	27
Total		203	224
Hydrogen bond donors		0	0
Torsion angles	ϕ	8	6

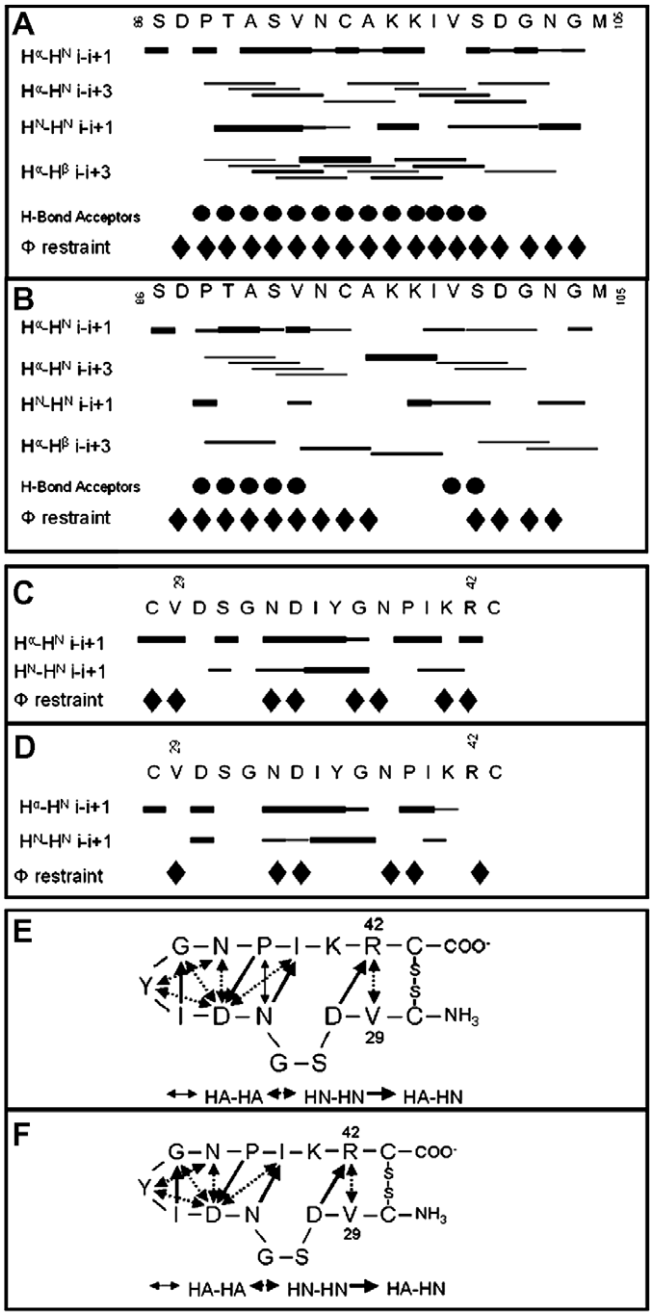

Fig. 4. Schematic of NOE contact types, hydrogen bond acceptors and residues giving rise to ϕ restraints for both the unmodified (A) and glycated (B) lysozyme helix 4 peptides, and the unmodified (C) and glycated (D) TIMP-2 AB β-hairpin peptides are shown. The width of the lines indicates the relative strength of the observed NOEs as determined from the number of contour lines. The backbone medium range NOEs observed in the TIMP-2 AB β-hairpin unmodified (E) and modified (F) peptides are also depicted.

Table 5
Summary of the rms deviation values for lysozyme helix 4 and TIMP-2 AB P β-hairpin

Peptide(s)	Region	rmsd
Lysozyme helix 440 structures	86–105	0.728
	86–104	0.628
Amadori lysozyme Helix 440 structures	86–105	2.252
	86–104	2.073
	86–95	0.487
	99–105	0.482
Helix 4 cf Amadori Helix 4 80 structures	86–105	1.687
	87–104	1.503
	86–95	0.491
	99–104	0.362
Lysozyme helix 4 peptide cf Helix from intact protein 40 + 1 structures	87–104	0.653
TIMP-2 P β-hairpin 30 structures	Cys 1–Cys2	1.718
	29–42	1.373
	30–41	1.150
TIMP–2 P β-hairpin cf TIMP-2 P β-hairpin from intact protein 30 + 1 structures	29–42	1.668
Amadori TIMP-2 P β-hairpin 30 structures	Cys1–Cys2	2.173
	29–42	1.690
	30–41	1.320
TIMP-2 P β-hairpin cf Amadori TIMP-2 P β-hairpin 60 structures	Cys1-Cys2	2.093
	29–42	1.668
	30–41	1.317
TIMP-2 P β-hairpin cf Amadori TIMP-2 P β-hairpin cf TIMP-2 1 + 1 + 1 structures	29–42	1.330
	30–41	1.073

Comparison of values for peptides before and after modification are shown together with comparisons to the equivalent region of the intact protein.

are close to other amino groups (Iberg and Flückiger, 1986). From our previous study using an HSA model peptide, we predict that no secondary structure is present in aqueous PBS solution in the absence of TFE (the conditions under which glycation is performed) and therefore while accessibility may explain the preferential glycation in the intact protein, local acid-based catalysis must give rise to the specificity in this case. Those amino acids neighboring each of the lysine residues must result in Lys^{97} being more nucleophilic than Lys^{96} and explaining its preferential glycation. Glycation of Lys^{97} may in turn lead to steric hindrance of Lys^{96}, limiting or preventing the formation of diglycated adducts whereby Lys^{96} and Lys^{97} would both be modified.

As in many peptide studies we utilized 2,2,2-trifluoroethanol (TFE) in order to drive the formation of, and stabilize, the lysozyme helix 4 model peptide as it is well documented that many peptides do not have a propensity to form helical secondary structure in the absence of such agents (Howard and Smales, 2005). The control lysozyme helix 4 peptide formed a typical α-helix in the presence of 30% (v/v) TFE that was consistent with the equivalent helix in the intact protein (Fig. 5). On-the-other-hand, NMR analysis of the glycated lysozyme helix 4 peptide in the presence of 30% (v/v) TFE shows that the helical nature of the peptide is severely disrupted immediately around the site of modification (Fig. 5). Further, the region around the modification showed a large amount of flexibility in the

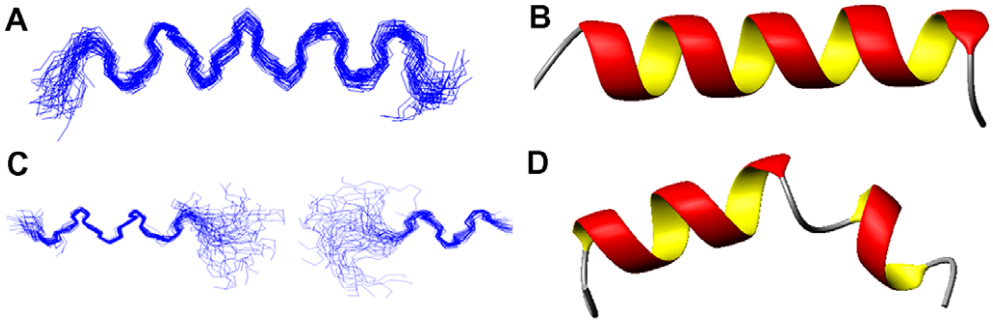

Fig. 5. Superimposition of all backbone heavy atoms of the 40-structure ensembles calculated from NMR data for lysozyme helix 4 unmodified (A) and ribbon diagram created in MOLMOL of the structure closest to the mean is shown for the unmodified (B). Superimposition of all backbone heavy atoms of the 40-structure ensembles calculated from NMR data for glycated lysozyme helix 4 residues 86–101 fitted over residues 86–95, and residues 95–105 fitted over residues 99–105 (C). Ribbon diagram created in MOLMOL of the structure closest to the mean is shown for the glycated peptide (D). We stress that figure (D) represents the structure closest to the mean and does not imply that the orientation of the two helical portions are actually constrained in the manner shown.

Table 6
Average ensemble energies (kJ mol^{-1}) for calculated structures of both unmodified and glycated lysozyme peptide obtained from DEEPVIEW using GROMOS9643B1

Energy	Unmodified	Glycated	Helix from Lysozyme 1E8L.pdb
Bonds	13.40	12.66	2.20
Angles	53.84	58.50	55.10
Torsions	135.29	157.39	140.60
Impropers	15.89	21.56	17.30
Nonbonded	−325.60	−267.43	−272.50
Total (kJmol^{-1})	−107.18	−17.32	−38.30

Energies for the equivalent helix within lysozyme structure lE8L.pdb are also shown for comparison.

Table 7
Average ensemble energies (kJmol^{-1}) for calculated structures of both unmodified and glycated TIMP-2 peptide obtained from DEEPVIEW using GROMOS9643B1

Energy	Unmodified	Glycated	2TMP.pdb
Bonds	12.90	17.60	12.70
Angles	41.20	69.00	50.00
Torsions	125.60	128.70	102.30
Impropers	14.70	14.40	16.50
Nonbonded	−261.60	−142.01	−167.20
Total (kJ mol^{-1})	−67.20	87.69	14.3

Energies for the equivalent region within TIMP-2 structure 2TMP.pdb are also shown for comparison.

glycated peptide and did not adopt one fixed conformation (Fig. 5), suggesting that glycation of Lys^{97} not only disrupts, but completely destroys, the interactions maintaining the helix in this region. It is the loss of structural NOE contacts that leads to this conclusion. Interestingly, the remainder of the helical structure at each end of the peptide remains unchanged upon glycation and it is only in the immediate vicinity of the modification that the helicity of the peptide is compromised (Fig. 5). We therefore suggest that glycation of Lys^{97} destroys the helical nature of the peptide within this region due to an enthalpy effect, whereby the presence of the attached sugar moiety leads to the disruption of the local non-covalent interactions stabilizing the helix in this area. We note that CD analysis of the control and glycated peptides in TFE also confirmed the presence of helical structure in both cases, and whilst there was some change between the two spectra we were unable to draw any further conclusions based upon this data as to how or where the helical structure may have been disrupted (data not shown).

The finding that glycation of the lysozyme helix 4 peptide disrupts the helical nature of the peptide is consistent with our previous findings using an HSA model helix forming peptide (Howard and Smales, 2005). As mentioned above, glycation of the lysozyme peptide leads to completely disordered structure in the region of the modified lysine residue whilst the glycated HSA peptide maintained ordered structure around the region of modification. In the glycated HSA peptide, NOE contacts between the protons in the sugar moiety and the surrounding amino acid residue protons were clearly observed, forcing and stabilizing the distorted helical structure observed (Howard and Smales, 2005). In the current study, however, there are no observable NOE contacts between the attached sugar moiety and the peptide, leaving the sugar relatively flexible. Thus, whilst modification of the peptide disrupted the local secondary structure of the lysozyme peptide, the lack of interactions between the sugar moiety and the peptide means that no conformation is preferred. A similar effect was reported upon glycation of the C-terminal region of α-crystallin protein (Blakytny et al., 1997) where no NOEs were observed between the sugar moiety and the peptide. Blakytny and colleagues showed that the exact sites and level of glycation could be identified, but the sugar did not stabilize a preferred structure in solution (Blakytny et al., 1997).

Our studies, and that of Blakytny and colleagues show that the local environment, in terms of amino acid sequence, not only plays an important role in determining

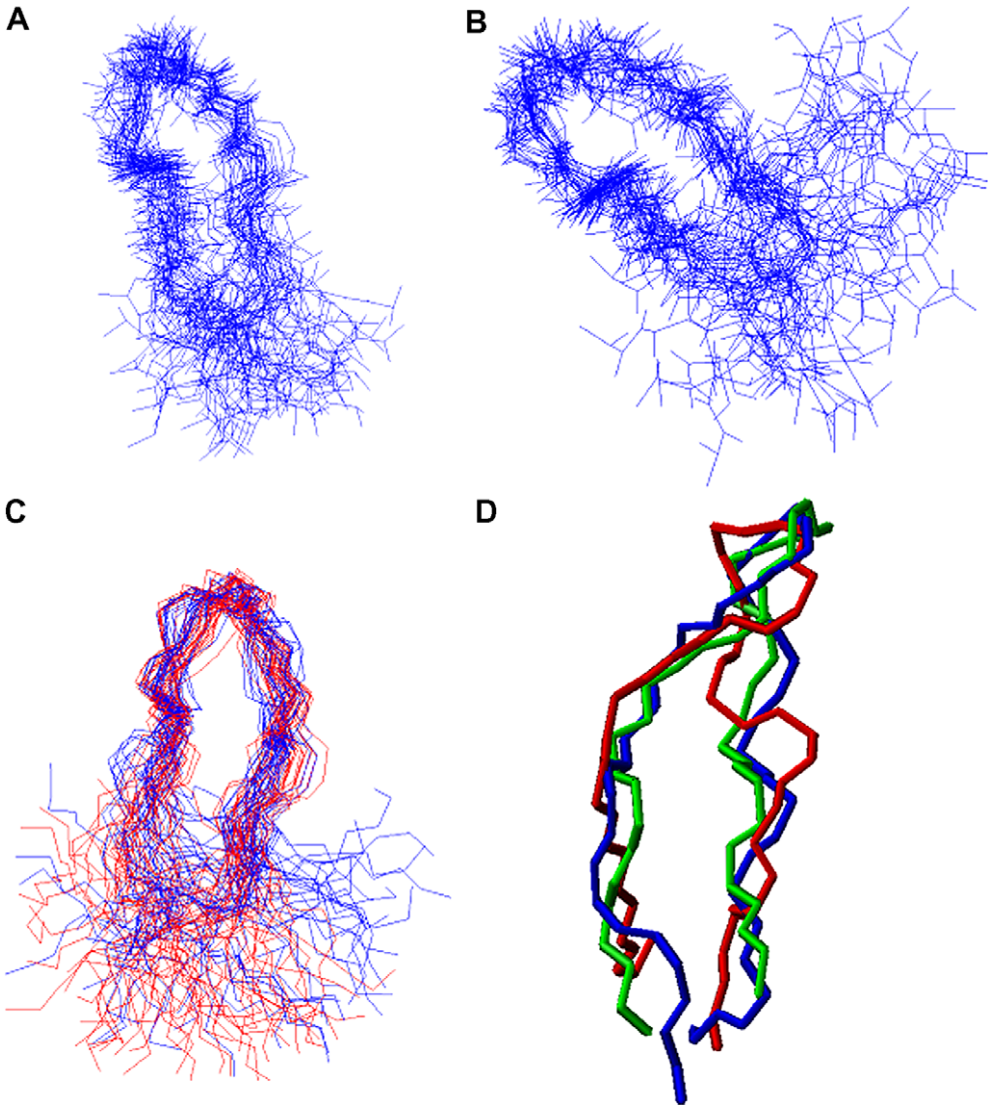

Fig. 6. Superimposition of all backbone heavy atoms of the 30-structure ensembles calculated from NMR data for unmodified TIMP-2 AB β-hairpin peptide (A) and "modified" TIMP-2 β-hairpin peptide (B). Superimposition of all backbone heavy atoms of the 60-structure ensembles calculated from NMR data for unmodified TIMP-2 β-hairpin peptide and "modified" peptide together (C). Superimposition of the structures closest to the mean for unmodified TIMP-2 β-hairpin peptide (blue) and "modified" TIMP-2 β-hairpin (red) peptides and the equivalent region of intact TIMP-2 (green) (D).

which lysine residue in a dilysine motif is glycated, but also plays a key role in determining whether such a modification leads to ordered or disordered secondary structure. In the absence of interactions between the sugar residue and the peptide backbone the local structure will be disordered, however, if nearby amino acids provide suitable partners for interactions with the sugar moiety a preferred structure will be adopted as in the case of the HSA model peptide. We note that in the case of the intact protein additional, interactions between the helix and the bulk protein that stabilize the helix are likely to be important in terms of the gross effect of glycation upon the helix structure. It is also interesting to note that previous studies have suggested that glycation of human serum albumin can lead to conformation change (Shaklai et al., 1984), although to our knowledge there have been no reports on the effect of glycation on lysozyme protein secondary and/or tertiary structure.

There was only a relatively weak 'sugar box' observed in the TOCSY NMR spectra of the TIMP-2 AB β-hairpin after modification suggesting that very little glycation of the peptide had taken place. There is only one lysine residue in the TIMP-2 AB β-hairpin, which may explain the relatively low reactivity of this residue compared to those in dilysine motifs. Even if there was modification, as the lysine residue is towards the end of the peptide, any local disruption in this area that is already less ordered may not be apparent. These results suggest that either (a) the single lysine residue within the peptide is relatively unreactive and hence engineering dilysine motifs to single lysines could be an approach to limit glycation, or (b) that glycation of lysine residues towards the termini of secondary structures does not appreciably perturb the secondary structure, although further work needs to be carried out in other amino acid positions to confirm this. We cannot

rule out the possibility that the disulfide bond in the hairpin, which is necessary to maintain the hairpin structure, may prevent destabilization or structural perturbation upon glycation of the peptide.

In summary we have shown that glycation of model helical peptides results in local disruption of secondary structure, and that the secondary structure adopted upon glycation is dependent upon whether the attached sugar moiety forms stable interactions with the peptide itself. We also provide evidence that the resulting effect of glycation upon structure is sequence specific and determined by the local environment. These findings, and the structural consequences, will allow us to interrogate the local environment in other peptides and proteins to predict the likelihood of glycation, and then model the potential effect such modification might have upon structure/function. Such information will be useful in helping to develop biotherapeutic and food bioprocessing strategies that limit such potentially damaging reactions and structural distortions upon modification to maintain protein integrity. Further, in the case of recombinant biopharmaceuticals, it may be possible to engineer the protein to remove potentially reactive lysine resides without compromising the structure and function of the target protein. Finally, the fact that glycation can result in structural changes is likely to help improve our understanding of disease pathologies involving aggregation (e.g. transmissible neurodegenerative diseases) where glycation is known to occur (Choi et al., 2004).

Acknowledgments

We wish to thank Mrs. Judy Hardy and Mr. Kevin Howland, Biomolecular Analysis Facility, Department of Biosciences, University of Kent, for synthesizing the peptides used in this study. This work was supported by Grant BB/C504600/1 from the Biotechnology and Biological Sciences Research Council (BBSRC), UK.

References

Al-Abed, Y., Kapurniotu, A., Bucala, R., 1999. Advanced glycation end products: detection and reversal. Methods Enzymol. 309, 152.

Blakytny, R., Carver, J.A., Harding, J.J., Kilby, G.W., Sheil, M.M., 1997. A spectroscopic study of glycated bovine alpha-crystallin: investigation of flexibility of the C-terminal extension, chaperone activity and evidence for diglycation. Biochim. Biophys. Acta: Protein Struct. Mol. Enzymol. 1343, 299–315.

Brunger, A.T., Adams, P.D., Clore, G.M., DeLano, W.L., Gros, P., Grosse-Kunstleve, R.W., Jiang, J.S., Kuszewski, J., Nilges, M., Pannu, N.S., Read, R.J., Rice, L.M., Simonson, T., Warren, G.L., 1998. Crystallography & NMR system: a new software suite for macromolecular structure determination. Acta Crystallogr. D: Biol. Crystallogr. 54, 905–921.

Bucala, R., 1996. Laboratory evaluation of advanced glycosylation end products: relevance to diabetes, aging, and renal failure. Diagn. Endocrinol. Metab. 14, 99–106.

Choi, Y.G., Kim, J.I., Jeon, Y.C., Park, S.J., Choi, E.K., Rubenstein, R., Kascsak, R.J., Carp, R.I., Kim, Y.S., 2004. Nonenzymatic glycation at the N terminus of pathogenic prion protein in transmissible spongiform encephalopathies. J. Biol. Chem. 279, 30402–30409.

Cohen, M.P., 2003. Intervention strategies to prevent pathogenic effects of glycated albumin. Arch. Biochem. Biophys. 419, 25–30.

Davis, P.J., Smales, C.M., James, D.C., 2001. How can thermal processing modify the antigenicity of proteins? Allergy 56, 56–60.

Delaglio, F., Grzesiek, S., Vuister, G.W., Zhu, G., Pfeifer, J., Bax, A., 1995. NMRPipe: a multidimensional spectral processing system based on UNIX pipes. J. Biomol. NMR 6, 277–293.

Guex, N., Peitsch, M.C., 1997. SWISS-MODEL and the Swiss-PdbViewer: an environment for comparative protein modeling. Electrophoresis 18, 2714–2723.

Howard, M.J., Smales, C.M., 2005. NMR analysis of synthetic human serum albumin alpha-helix 28 identifies structural distortion upon amadori modification. J. Biol. Chem. 280, 22582–22589.

Iberg, N., Flückiger, R., 1986. Nonenzymatic glycosylation of albumin in vivo. Identification of multiple glycosylated sites. J. Biol. Chem. 261, 13542–13545.

Johnson, B.A., Blevins, R.A., 1994. NMR view—a computer program for the visualization and analysis of NMR data. J. Biomol. NMR 4, 603–614.

Koradi, R., Billeter, M., Wuthrich, K., 1996. MOLMOL: a program for display and analysis of macromolecular structures. J. Mol. Graph. 14, 51–55.

Laskowski, R.A., Rullmannn, J.A., MacArthur, M.W., Kaptein, R., Thornton, J.M., 1996. AQUA and PROCHECK-NMR: programs for checking the quality of protein structures solved by NMR. J. Biomol. NMR 8, 477–486.

Mendez, D.L., Jensen, R.A., McElroy, L.A., Pena, J.M., Esquerra, R.M., 2005. The effect of non-enzymatic glycation on the unfolding of human serum albumin. Arch. Biochem. Biophys. 444, 92–99.

Muskett, F.W., Frenkiel, T.A., Feeney, J., Freedman, R.B., Carr, M.D., Williamson, R.A., 1998. High resolution structure of the N-terminal domain of tissue inhibitor of metalloproteinases-2 and characterisation of its interaction site with matrix metalloproteinase-3. J. Biol. Chem. 273, 21736–21743.

Povey, J., Smales, C.M., Hassard, S., Howard, M.J., 2007. Comparison of the effects of 2,2,2-trifluoroethanol on peptide and protein structure and function. J. Struct. Biol. 157, 329–338.

Shaklai, N., Garlick, R., Bunn, H., 1984. Nonenzymatic glycosylation of human serum albumin alters its conformation and function. J. Biol. Chem. 259, 3812–3817.

Smales, C.M., Pepper, D.S., James, D.C., 2000. Protein modification during antiviral heat bioprocessing. Biotechnol. Bioeng. 67, 177–188.

Smales, C.M., Pepper, D.S., James, D.C., 2002. Protein modification during anti-viral heat-treatment bioprocessing of factor VIII concentrates, factor IX concentrates, and model proteins in the presence of sucrose. Biotechnol. Bioeng. 77, 37–48.

Stitt, A., 2001. Advanced glycation: an important pathological event in diabetic and age related ocular disease. Br. J. Ophthalmol. 85, 746–753.

Suarez, G., Rajaram, R., Oronsky, A.L., Gawinowicz, M.A., 1989. Nonenzymatic glycation of bovine serum albumin by fructose (fructation)—comparison with the Maillard reaction initiated by glucose. J. Biol. Chem. 264, 3674–3679.

Tagami, U., Akashi, S., Mizukoschi, T., Suzuki, E., Hirayama, K., 2000. Structural studies of the Maillard reaction products of a protein using ion trap mass spectrometer. J. Mass Spectrom. 35, 131–138.

van Gunsteren, W.F., Brunne, R.M., Gros, P., van Schaik, R.C., Schiffer, C.A., Torda, A.E., 1994. Accounting for molecular mobility in structure determination based on nuclear magnetic resonance spectroscopic and X-ray diffraction data. In: Janes, T.L., Oppenheimer, N.J. (Eds.), Methods in Enzymology: Nuclear Magnetic Resonance, vol. 239. Academic Press, New York, pp. 619–654.

Yeboah, F.K., Alli, I., Yaylatan, V.A., Yasuo, K., Chowdhury, S.F., Purisima, E.O., 2004. Effect of limited solid-state glycation on the conformation of lysozyme by ESI-MSMS peptide mapping and molecular modeling. Bioconjug. Chem. 15, 27–34.